Photochemical and Electrochemical Oxidation Reactions of Surface-Bound Polycyclic Aromatic Hydrocarbons

Maciej Mazur[†] **and G. J. Blanchard***[,‡]

Laboratory of Electrochemistry, Department of Chemistry, University of Warsaw, 02-093 Warsaw, Pasteura 1, Poland, and Department of Chemistry, Michigan State University, East Lansing, Michigan 48823-1322

Received: November 7, 2003

We have studied the oxidation reactions of two polycyclic aromatic hydrocarbons (PAHs), pyrene and anthracene, attached covalently to silica, indium-doped tin oxide (ITO), and gold surfaces. Attachment of the PAHs to the substrates was accomplished by established covalent coupling methods. For both pyrene and anthracene, we find that electrochemical and photochemical oxidation produces first a monohydroxy-PAH followed by the formation of dihydroxy/dione derivatives. We have used cyclic voltammetry and steady-state excitation and emission spectroscopy to identify the products of the surface reactions. The uniformity of our results for two chromophores and three different types of substrates demonstrates the generality of our findings and rules out the involvement of surface enhancement phenomena in these processes.

Introduction

The design and synthesis of monomolecular assemblies on solid substrates has drawn much interest in recent years due to the numerous potential applications of this class of materials in areas ranging from chemical separations to nonlinear optics and biosensor devices. The ability to manipulate the chemical structure of surfaces with molecular depth resolution provides a means to control properties such as friction, wetting, adhesion, electron transfer, and corrosion protection.[1−5] A testament to the strength of this research endeavor is the structural diversity in deposition chemistry that has appeared. Monomolecular layers can be prepared by a variety of methods, including Langmuir−Blodgett deposition,[6,7] spontaneous self-assembly,[8,9] ionic[10−13] and covalent binding,[14,15] and polyelectrolyte layer deposition.[16−23]

The most widely studied and, arguably, the best characterized monomolecular assemblies are alkanethiols on gold.[3,5,24,25] Our interest in monolayer and multilayer structures lies in their utility for chemical and biosensing applications. Because thiol monolayers are limited to forming on metallic substrates such as gold, silver, copper, and mercury and a few semiconductor surfaces,[26,27] other approaches to the formation of adlayers on different substrates are required. Films of silanes,[28] fatty acids,[8,9] phosphonates,[10−13] and acid chlorides[15,29] have been demonstrated on both conductive and insulating substrates, providing a rich variety of chemistry from which to construct interfaces useful for sensing.

To effect chemical sensing, it is necessary to incorporate some means of signal transduction into the interface. Our group has incorporated optical chromophores into monolayer and multilayer assemblies, and we have used steady-state, time-resolved and nonlinear optical spectroscopies to interrogate these imbedded chromophores. We have found that the identity and functionality of the incorporated chromophore can have a significant influence on the information acquired. In some cases we have found that the chromophores are not stable to UV exposure under ambient atmospheric conditions, and it is important that we elucidate the chemical and/or physical basis for this behavior so that it can be avoided when possible.

We report here on the covalent binding of pyrene and anthracene derivatives to silica, gold, and ITO substrates. Pyrene is used frequently as a polarity-sensitive probe to study relaxation dynamics in bulk solvents[30] and in a variety of adlayers.[31] Though anthracene has seen much less use as an optical probe, it is structurally different from pyrene and thus represents a useful system for comparison. An important limitation to the use of PAHs as optical probes is their chemical instability. To this point, it has been unclear whether this instability is surface enhanced or not, and a significant issue we consider here is the generality of the propensity of PAHs to degrade at surfaces. There is some literature precedent for photooxidation of PAHs. Pyrene and anthracene physisorbed to various substrates transform into a number of products, mainly alcohols and ketones, when exposed to oxygen and UV light.[32−36] We are interested in the influence of the substrate and whether this effect is dominated by the presence of UV photons and oxygen or requires both to operate. Our data point to similar photooxidation behavior for both pyrene and anthracene bound covalently to conducting, semiconducting, and insulating substrates. We identify the oxidation products of these PAHs using emission spectroscopy and cyclic voltammetry. Our data point to similar chemistry being operative for both PAHs bound to different surfaces. If there is indeed any surface-enhancement effect, it arises solely from the proximity of the bound PAHs to any adventitious water physisorbed to the surface. The degradation of surface-bound pyrene and anthracene requires the presence of both UV light and oxygen.

Experimental Section

Chemicals. All chemicals were of the highest quality commercially available: 1-aminopyrene (Aldrich, >98%), 1-aminoanthracene (Aldrich, 90%), adipoyl chloride (Aldrich, 98%), 4-methylmorpholine (Aldrich, 99%), 1-hydroxypyrene (Aldrich,

* Corresponding author. E-mail: Blanchard@chemistry.msu.edu.
[†] University of Warsaw.
[‡] Michigan State University.

10.1021/jp037393j CCC: $27.50
Published on Web 12/18/2003

98%), 1,6-pyrenedione (Aldrich), pyrene (Aldrich, 99%), 1,4-anthracenedione (Aldrich), 9,10-anthracenedione (Aldrich), 11-mercaptoundecanoic acid (MUA) (Aldrich, 95%), triethylamine (Aldrich, 99.5%), acetic anhydride (CCI, ACS grade), sodium borohydride (Aldrich, 98%), methylene blue (Fluka, 97%), acetonitrile (Aldrich, anhydrous, 99.8%), ethyl acetate (Spectrum Chemical, ACS grade), ethanol (Aldrich, ACS grade), sulfuric acid (Aldrich, 99.999%), 1-pentanol (Aldrich, 99+%). Aqueous solutions were prepared from water distilled in-house.

Steady-State Emission Spectroscopy. Emission and excitation spectra were recorded with a Spex Fluorolog 3 spectrometer using a 3 nm band-pass for excitation and a 3 nm band-pass for emission collection.

Electrochemical Measurements. Electrochemical measurements were conducted with a PC-controlled Electrochemical Workstation (CH Instruments Model 650A), using a small volume three-electrode cell with Pt wire as the counter electrode. All potentials are quoted versus a Ag/AgCl/1 M KCl_{aq} reference electrode.

Substrate Preparation. Quartz slides (NSG Precision Cells, Inc., P/N 10040 UV fused silica windows, nonfluorescent) and gold electrodes (Au, 99.99%; 0.2 cm^2) were cleaned by immersion in piranha solution for ca. 20 min. ***Caution!*** **Piranha solution reacts violently with organic matter and should be handled with extreme care!** Indium-doped tin oxide (ITO) films (Bayview Optics, Dover-Foxcroft, ME) deposited on the same quartz slides were used for spectroscopic measurements and ITO films on glass substrates (Delta Technologies) were used for electrochemical measurements.

Bonding 1-Aminopyrene and 1-Aminoanthracene to Quartz and ITO. Quartz and ITO substrates were reacted with adipoyl chloride (0.3 mL) in dry acetonitrile (10 mL), using 4-methylmorpholine (0.3 mL) as a Lewis base, under reduced pressure for 1 h. The reacted substrates were removed from the reaction vessel, rinsed with dry acetonitrile and ethyl acetate, and dried under a stream of nitrogen. Then the acid chloride terminal functionalities were reacted with either 1-aminopyrene or 1-aminoanthracene by exposing substrates with an adipoyl chloride adlayer to a 30 mM solution of the amino-substituted PAH in dry acetonitrile for 1 h. The substrates were then removed from the reaction vessel, washed with dry acetonitrile and ethyl acetate, and dried under a stream of nitrogen.

Bonding 1-Aminopyrene and 1-Aminoanthracene to Gold. Monolayers of 11-mercaptoundecanoic acid (MUA) were prepared by immersing clean gold substrates into 10 mM MUA in acetonitrile solution for 4 h. Then, the monolayer-modified gold surface was removed from the solution, rinsed with acetonitrile and dried. The terminal carboxylic acid groups were then transformed into interchain anhydrides,[37] by placing the substrate in a solution of acetic anhydride (0.3 mL) and triethylamine (0.3 mL) in dry acetonitrile (10 mL) for 1 h. The reacted substrates were removed from the reaction vessel, rinsed with dry acetonitrile and ethyl acetate, and dried under a stream of nitrogen. The acid anhydride terminal functionalities were reacted with either 1-aminopyrene or 1-aminoanthracene by exposing the anhydride-terminated substrates to a 30 mM solution of the amino-substituted PAH in dry acetonitrile for 1 h. The substrates were then removed from the reaction vessel, washed with dry acetonitrile and ethyl acetate, and dried under a stream of nitrogen.

Preparation of Thin Films of Bipyrene, 1-Hydroxypyrene, 1,6-Pyrenedione, 1,4-Anthracenedione, and 9,10-Anthracenedione on Gold. Thin films of bipyrene on gold were prepared electrochemically according to the procedure developed by Zotti et al.[38] for the oxidation of pyrene in dry acetonitrile solution. 1-Hydroxypyrene, 1,6-pyrenedione, 1,4-anthracenedione, and 9,10-anthracenedione thin films on gold were prepared by immersing the substrates into acetonitrile solution (50 mM) of the compound, then removed from the solution, and allowed to dry. The modified electrodes were then subjected to electrochemical characterization in aqueous solution.

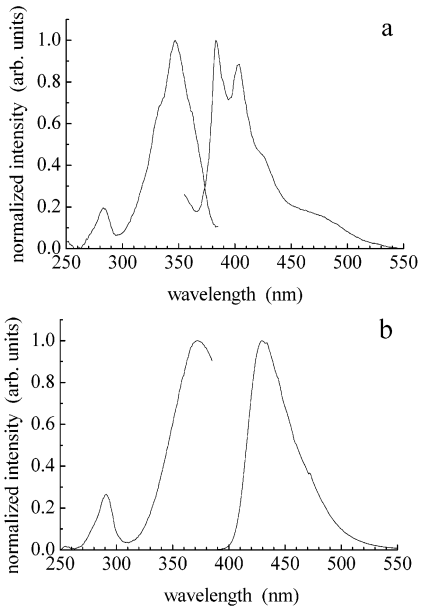

Figure 1. (a) Excitation and emission spectra of aminopyrene attached to an adipoyl chloride adlayer on quartz and (b) aminopyrene solution phase spectra taken in 1-pentanol.

Preparation of 1,6-Dihydroxypyrene. 1,6-Dihydroxypyrene was prepared by reduction of 2 mL of 10^{-4} M 1,6-pyrenedione in 1-pentanol with 2 mL of saturated sodium borohydride in 1-pentanol.

Preparation of Amidoanthracene Acetate. 1-Aminoanthracene (0.2 g) was reacted with excess acetic anhydride (15 mL) in dry acetonitrile (15 mL) for ca. 20 h. The reaction mixture was poured into distilled water, which resulted in precipitation of amidoanthracene acetate. The product was then collected by filtration on a separation funnel (80% yield).

Determination of Reactivity with Singlet Oxygen. Substrates with bound PAHs were immersed in a solution of methylene blue in ethanol (ca. 1 mM) for several seconds, then removed from solution, allowed to dry, and exposed to 650 nm light (20 h, ~7 mW/cm^2). The red-irradiated samples were immersed in ethanol to remove physisorbed methylene blue, then rinsed with ethanol, dried, and examined for the presence of PAHs degradation products using emission spectroscopy.

Results and Discussion

The goal of this work is to understand the basis for the observed degradation of PAHs bound to surfaces. Either UV light or electrochemical oxidation in the presence of ambient O_2 can play a role in the degradation, with the characteristic formation of mono- and dihydroxy and dione derivatives of the PAHs resulting. Because the structures, and spectroscopic and electrochemical responses, of the two PAHs we report on are significantly different, we consider our results for surface-bound pyrene and anthracene species separately.

Pyrene. We have investigated pyrene bound covalently to quartz by emission spectroscopy. We show in Figure 1a the excitation and emission spectra of aminopyrene after covalent bonding to a quartz substrate to form an amidopyrene. The

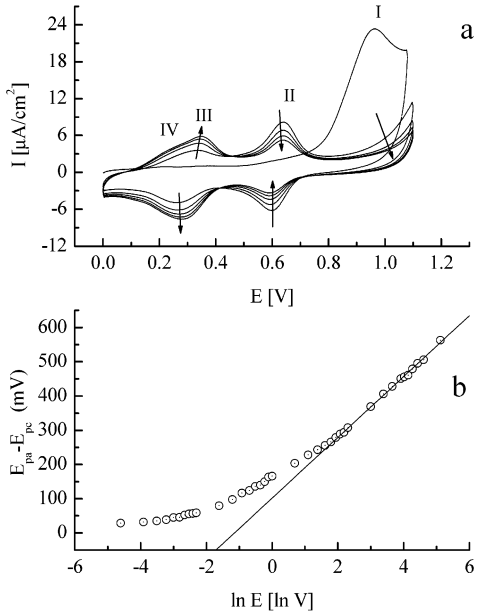

Figure 2. (a) Cyclic voltammograms of 11-(1-amidopyrenyl)-1-mercaptoundecanoate on gold in aqueous 0.5 M H_2SO_4. Sweep rate: 0.1 V/s. (b) Dependence of the separation of anodic and cathodic peak potentials for redox pair III as a function of the logarithm of sweep rate.

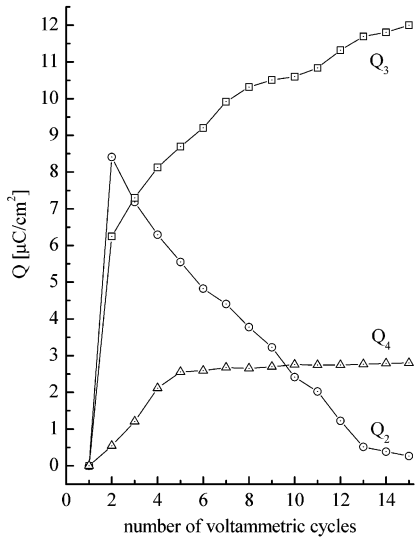

Figure 3. Dependence of charges under voltammetric peaks for species II, III, and IV as a function of number of CV scans.

excitation spectrum reveals two bands with maxima at 283 and 347 nm, both associated with the surface-bound pyrene.

The emission spectrum shows two bands, with maxima at 385 and 405 nm. The spectra are very similar to those of 1-acetamidopyrene in pentanol[39] and are significantly different from the solution phase spectra of 1-aminopyrene (Figure 1b). These data indicate that the immobilized pyrene is bound covalently to the surface through an amide bond. It should be noted that we do not observe any significant band in the 450−500 nm range, which would indicate excimer emission. This finding may be the result of a relatively low surface concentration of pyrene molecules or their hindered mobility due to covalent binding to the substrate. The latter case is more likely because the formation of excimers was observed even at low surface concentrations of pyrene physisorbed on silica.[40]

We have also examined the susceptibility of bound pyrene to electrochemical oxidation using cyclic voltammetry. We show in Figure 2a a series of voltammetric scans for amidopyrene bound covalently to gold. In the first scan, when the anodic potential above ca. 0.8 V is applied to the electrode, we observe an irreversible peak with a maximum at 0.96 V. For the reverse scan and in subsequent scans, a number of new redox peaks appear in voltammograms. These are a pair of peaks at 0.62 V (designated II in Figure 2a) and two pairs at 0.21 V (IV) and 0.32 V (III). We assign the irreversible peak at 0.96 V to oxidation of pyrene and the consequent formation of radical cations. Because radical cations are highly reactive, we do not observe a reduction peak; the radical cations undergo rapid reaction to more stable species. We see that the peak pair II is associated with an intermediate species on the basis of the observation that the magnitude of these peaks decreases monotonically in consecutive scans. In contrast, peaks III and IV increase in magnitude with the number of scans, appearing to be the final products of pyrene oxidation.

Due to the complexity of this system, a detailed analysis of the electrochemical data is difficult. Accordingly, we have analyzed in detail only the redox reaction of the stable species III in Figure 2a. We recorded a set of voltammetric curves varying sweep rate and plotted the separation of the anodic and cathodic peak potentials as a function of the logarithm of the sweep rate (Figure 2b). On the basis of the theory proposed by Laviron,[41] from the slope of the linear portion of the curve we were able to determine the value of the transfer coefficient α and the number of electrons involved in the redox reaction. We obtain reasonable values of α ($0 < \alpha < 1$) only for a two-electron reaction. Fitting these data to the theory with $n = 2$ yields a value of $\alpha = 0.2$.

On the basis of the voltammetric curves recorded on gold in aqueous solution, we can plot the values of charge exchanged in redox reactions for the species present on the surface during subsequent scans. The results are presented in Figure 3. The concentration (charge) of species II reaches its maximum value in the second scan, just after formation of radical cations in the first scan; then it gradually decreases, approaching zero after multiple cycles. At the same time, the charge associated with species III reaches the value of 6.2 mC/cm^2 in the second scan, and then increases monotonically to ~12 μC/cm^2. The concentration of species IV reaches 2.8 μC/cm^2 and remains approximately constant beyond five cycles.

We consider next the assignment of the species associated with these peaks. The degradation of physisorbed pyrene on various solid substrates has been established[32−35] and is usually explained in terms of the formation of reactive radical cations, which follow a variety of reaction pathways, including introduction of hydroxyl and carbonyl groups to the ring system, and dimerization. These findings provide a frame of reference for the assignment of the electrochemical features we see for surface-bound pyrene.

To identify the surface species, we have recorded cyclic voltammograms of a number of candidate compounds. Although we study physisorbed and not surface-bound molecules we believe the electrochemical behavior (formal potentials) in both cases is similar. We do not report on solution phase electrochemical behavior due to very low solubility of the studied compounds in water. We show in Figure 4a the voltammetric behavior of 1-hydroxypyrene adsorbed to a gold electrode. In the first scan we observe an irreversible peak at 0.71 V, which is followed by the formation of a new product with peaks at ~0.32 V. In subsequent scans, the peak at 0.71 V diminishes rapidly, indicating hydroxypyrene is transformed into a new product. We note that the oxidation peak potential of 1-hy-

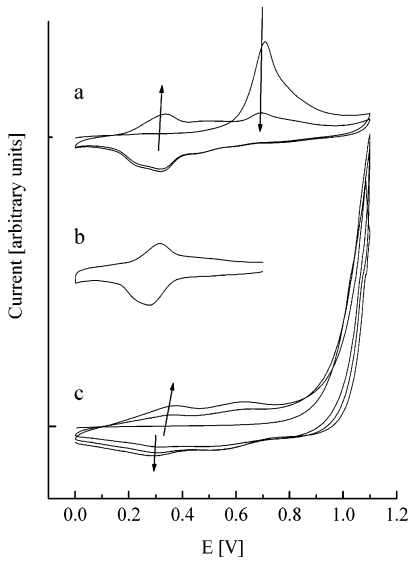

Figure 4. Cyclic voltammograms of thin layers of (a) 1-hydroxypyrene, (b) 1,6-pyrenedione, and (c) bipyrene deposited on gold in aqueous 0.5 M H_2SO_4. The sweep rate was 0.1 V/s for all measurements.

droxypyrene (0.71 V, Figure 4a) is relatively close to the formal potential of the intermediate species II we see for covalently bound amidopyrene (0.62 V, Figure 2a). Both species II (Figure 2a) and hydroxypyrene are unstable and are transformed into a new product, producing peaks at ~0.32 V. We thus assign species II (Figure 2a) as a hydroxy derivative of surface-bound pyrene.

Figure 4b shows a cyclic voltammogram of the 1,6-pyrenedione/1,6-dihydroxypyrene redox couple. We note a pair of voltammetric peaks centered at 0.32 V, with the similarity of these signals to peaks III (Figure 2a) and products of hydroxypyrene oxidation (Figure 4a) being clear, and we conclude that the signals at 0.32 V in both Figures 2 and 4a are due to the 1,6-dihydroxy/dione derivative of pyrene.

We consider next the origin of peaks IV (Figure 2). It is possible that these peaks are associated with a dimeric species or an isomeric pyrenedione/dihydroxypyrene redox couple. Figure 4c shows voltammetric scans of a physisorbed bipyrene thin film on gold in aqueous solution. The increase in current above ca. 0.9 V can be assigned to oxidation of bipyrene. In subsequent scans the new products produce signals at 0.60, 0.34, and 0.25 V. On the basis of these data, none of signals II−IV (Figure 2) can be assigned to bipyrene species. However, the signals associated with the oxidation products of bipyrene are qualitatively similar to those for the oxidation products of surface-bound pyrene, suggesting that the oxidation of bipyrene in aqueous media produces a monohydroxy derivative (peak pair at 0.65 V) and a dihydroxy derivative (0.4 V). We also observe the third pair of peaks at 0.25 V and believe it to be a counterpart to species IV. Our data indicate that the electrochemical behavior of pyrene and bipyrene in aqueous medium is substantially the same.

The origin of peaks IV in Figure 2a remains to be established. Moriconi et al.[42] have reported that the standard potential of 1,8-pyrenedione/1,8-dihydroxypyrene is cathodically shifted ca. 100 mV with respect to the 1,6-pyrenedione/1,6-dihydroxypyrene couple. On the basis of this information, species IV is likely the 1,8-dihydroxy/1,8-dione derivative of pyrene.

The electrochemical data suggest the following scenario for pyrene reactions occurring at the electrode surface (Scheme 1). The anodic polarization of the electrode above 0.8 V results in the formation of pyrene radical cations. These radical cations

SCHEME 1 : Oxidation of Surface-Bound Pyrene

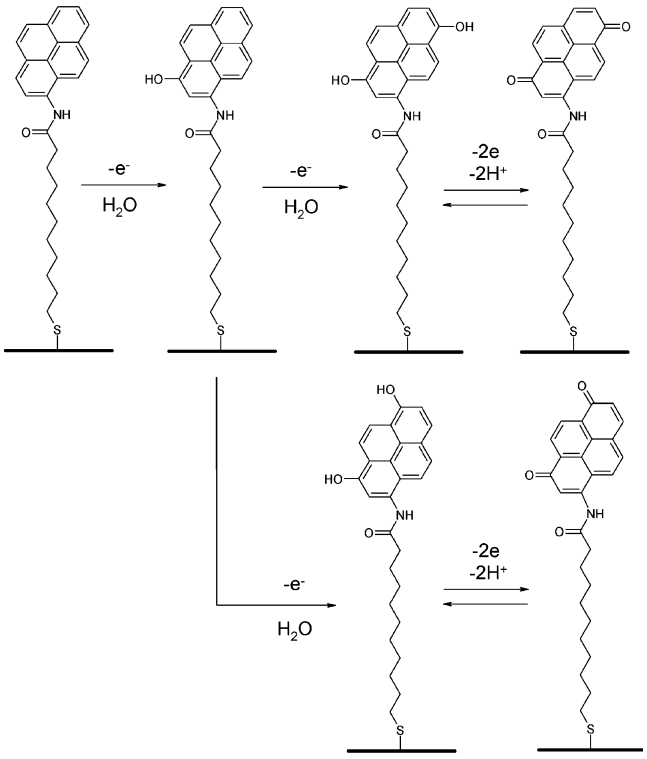

react with water to form a monohydroxy derivative. The monohydroxy derivative is further transformed by reaction with another water molecule to produce more than one isomeric form of dihydroxypyrene/pyrenedione. We cannot explicitly exclude the formation of dimeric (bipyrene) or oligomeric species that are subsequently transformed into hydroxyl/quinone derivatves, but this possibility seems less probable due to the expected changes in redox potential for the oligomers and the absence of experimental data pointing to additional species.

We can estimate the surface concentration of pyrene molecules on the basis of its electrochemical reaction, but due to complexity of the system we need to make some assumptions. We calculated the values of charge under voltmmetric peaks for the curves shown in Figure 2a. The Q_I value represents the total charge consumed by the oxidation of pyrene, oxidation of the formed monohydroxy derivative, and oxidation of dihydroxypyrenes. Assuming that all the pyrene molecules are transformed into mono- or dihydroxy derivatives by the second voltammetric scan, we get the charge associated (formally) with one- or two-electron oxidation of pyrene by calculating the value $Q_I - Q_{II} - Q_{III} - Q_{IV}$, where Q_{II}, Q_{III}, and Q_{IV} are the values of charge under voltammetric peaks taken from the second scan and Q_I is the value of charge under the voltammetric peak taken from the first scan. Thus, some fraction of the molecules after one-electron oxidation is transformed into the monohydroxy derivative and the rest (after two-electron oxidation) is transformed into dihydroxy derivative(s). We need therefore to estimate the fraction of molecules following the one- and two-electron processes. We can do this by calculating the values $2Q_{II}/(2Q_{II} + Q_{III} + Q_{IV})$ for the molecules experiencing one-electron oxidation and $(Q_{III} + Q_{IV})/(2Q_{II} + Q_{III} + Q_{IV})$ for those experiencing two-electron oxidation. The quantity $[Q_I - (Q_{II} + Q_{III} + Q_{IV})][2Q_{II}/(2Q_{II} + Q_{III} + Q_{IV})]/F$ gives the surface concentration of pyrene transformed into the monohydroxy derivative (in the second voltammetric scan) and $[Q_I - (Q_{II} + Q_{III} + Q_{IV})][(Q_{III} + Q_{IV})/(2Q_{II} + Q_{III} + Q_{IV})]/(2F)$ is the concentration of the molecules transformed into dihydroxy-

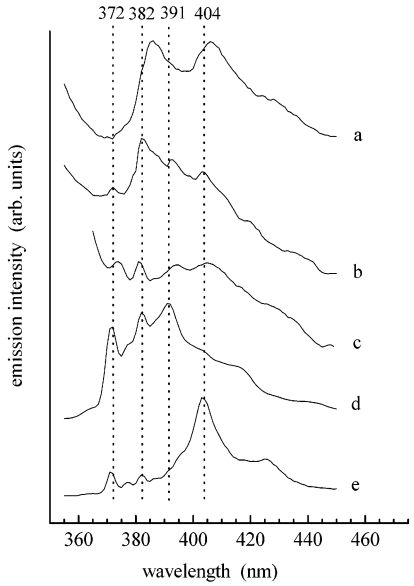

Figure 5. Emission spectra of (a) amidopyrenehexanoate bound to ITO, (b) products of the electrochemical oxidation of amidopyrenehexanoate bound to ITO, (c) products of the photochemical degradation of amidopyrenehexanoate bound to ITO, (d) 1,6-pyrenedione in 1-pentanol, and (e) 1,6-dihydroxypyrene in 1-pentanol.

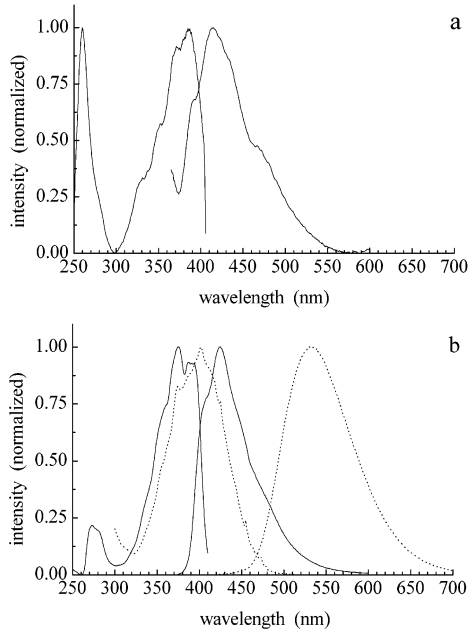

Figure 6. (a) Excitation and emission spectra of aminoanthracene attached to an adipoyl chloride adlayer on quartz. (b) Excitation and emission spectra of 1-amidoanthracene acetate (solid line) and 1-aminoanthracene (dotted line) dissolved in pentanol.

pyrene. The sum of these two terms gives us the total concentration of pyrene molecules according to the formula: $\Gamma = [Q_I - (Q_{II} + Q_{III} + Q_{IV})][2Q_{II} + (Q_{III} + Q_{IV})/2]/(2Q_{II} + Q_{III} + Q_{IV})/F = 2.1 \times 10^{-10}$ mol/cm^2. If we assume that the full monolayer corresponds to the concentration of alkanethiol molecules on gold, 7.7×10^{-10} mol/cm^2,[43] we achieve a surface coverage of pyrene moieties of ~27% of a monolayer. Because the pyrene attachment chemistry involves the use of two MUA surface-bound molecules, we achieve ~50% reaction efficiency for pyrene layer formation.

To study the emission spectra of covalently bound pyrene, we used ITO-coated silica substrates. The electrochemical behavior of pyrene on ITO is qualitatively similar to that on gold. We show in Figure 5 the emission spectra of pyrene bound covalently to ITO, before (a) and after (b) electrochemical oxidation in aqueous H_2SO_4. For non-oxidized pyrene we see two emission bands at 385 and 405 nm (similar to those seen on SiO_x, Figure 1). Following electrochemical oxidation, these bands shift slightly to 382 and 404 nm, and two new bands appear at 372 and 393 nm. We compare these spectra to that of 1,6-dihydroxypyrene (d) and 1,6-pyrenedione (e). The 1,6-dihydroxypyrene spectrum is characterized by three bands at 372, 382, and 391 nm, and we can find the same bands in the spectrum of the product of pyrene oxidation (b). The spectrum of 1,6-pyrenedione has a relatively intense band at 404 nm, coincident with the band seen in the spectrum of the electrochemically oxidized form.

Upon irradiation with UV light (340 nm, 20 h, ~7 mW/cm^2) and in the presence of atmospheric oxygen, the covalently bound pyrene is transformed into a species with emission bands at 373, 381, 394, and 405 nm (Figure 5c), bands characteristic of dihydroxypyrene and pyrenedione. This finding shows that both electrochemical oxidation and UV photolysis in the presence of oxygen result in the same products being formed. The difference in band ratios for electrochemical and photochemical oxidation suggest the presence of additional species resulting from exposure to UV light (Figure 5b,c). We observed that the photodegradation of surface-bound pyrene is much slower under nitrogen than in the presence of oxygen, underscoring the central role of oxygen and/or water in the degradation reactions.

Although the products of electrochemical or photochemical transformations are the same, the mechanism of each reaction may be different. In the case of electrochemical oxidation we did not observe any effect of oxygen dissolved in the solution on the voltammetric behavior. This finding means that oxygen does not play a role in surface reactions and the pyrene is simply oxidized through electron transfer from the molecule to the metal (or semiconductor). Then the oxidized molecule reacts with water to produce a monohydroxypyrene.

The photodegradation of pyrene can occur through two paths. The first is electron transfer between excited pyrene and O_2, resulting in formation of a pyrene radical cation and a superoxide (O_2^-). The pyrene radical can then react with water (physisorbed on the surface) to give the hydroxyl derivative.

The second mechanism by which photodegradation can occur is the reaction of pyrene with generated singlet oxygen. It is known that triplet oxygen may quench the excited states of pyrene, and this quenching process yields singlet oxygen. The singlet oxygen can react subsequently with pyrene by addition to the ring system.

To determine which of the mechanisms occur for our systems, we performed an experiment where we physisorbed methylene blue (a well-known singlet oxygen sensitizer) onto the substrate modified by covalent attachment of pyrene and excited the methylene blue at 650 nm in the presence of oxygen. The singlet oxygen formed by irradiation of methylene blue could react with surface-bound pyrene to yield hydroxy and/or carbonyl derivatives. From these experiments, we did not observe (using emission spectroscopy) any significant loss of pyrene or presence of its degradation products. We conclude therefore that singlet oxygen is not involved in the photochemical transformation of surface bound pyrene and the electron-transfer mechanism is dominant.

Anthracene. We show in Figure 6a the excitation and emission spectra of anthracene bound covalently to quartz. The excitation spectrum reveals one relatively broad band centered

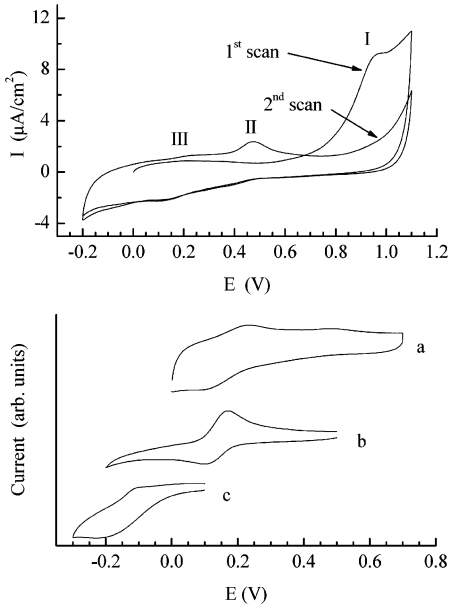

Figure 7. (a) Cyclic voltammograms in aqueous 0.5 M H_2SO_4 of 11-(1-amidoanthracenyl)-1-mercaptoundecanoate on gold. (b) (i) Steady-state CV of 11-(1-amidoanthracenyl)-1-mercaptoundecanoate on gold, (ii) a thin layer of 1,4-anthracenedione deposited on gold, and (iii) a thin layer of 9,10-anthracenedione deposited on gold.

at 380 nm, with the approximately mirror-image emission spectrum centered near 420 nm. These spectra are similar to those of amidoanthracene acetate recorded in solution (Figure 6b solid line) and significantly different form those of solution phase aminoanthracene (Figure 6b dotted line). These data confirm that the anthracene molecules are attached to the surface through an amide bond and are not simply physisorbed. The comparison of the spectrum of surface-bound anthracene (Figure 6a) and nonsubstituted anthracene[44] reveals the lack of vibronic structure on both the 380 nm absorption band and its corresponding emission band, centered near 430 nm. We obtain the same result for amidoanthracene acetate in the solution (Figure 6b) and conclude that these spectral changes are not the result of surface binding but are caused by the presence of the amido substituent on the anthracene ring system. We also do not observe any emission signals attributable to excimer formation, which is probably the result of covalent bonding of the chromophore to the substrate.

As with pyrene, anthracene bound covalently to SiO_x or ITO is not stable when exposed to UV light in the presence of atmospheric oxygen and water. Sample degradation is not observed when the sample is placed in the dark and is strongly attenuated when oxygen and water vapor are purged with nitrogen. To determine if the surface-bound anthracene moieties can be oxidized in a controlled manner, we bound aminoanthracene to a modified gold surface and examined the electrochemical behavior of the resulting interface. We show in Figure 7 a series of voltammetric curves for anthracene attached covalently to gold. In the first scan we observe an anodic peak at 0.95 V that is not associated with a cathodic peak when the polarization is reversed. This irreversible behavior suggests that anthracene is oxidized and then reacts rapidly to form a new product. The anthracene radicals generated by electrochemical oxidation most likely react with water molecules in a manner analogous to that seen for pyrene. This possibility is consistent with the electrochemical data, as seen in the second voltammetric scan, (Figure 7) where the peak at 0.95 V decreases and a new oxidation peak appears at 0.47 V. We assign this peak

SCHEME 2: Oxidation of Surface-Bound Anthracene

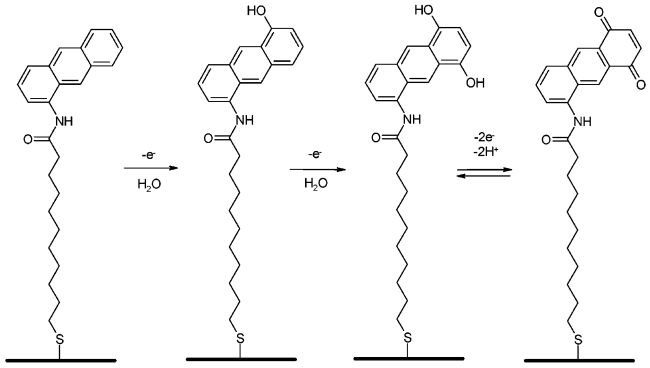

to the product of the reaction between the anthracene radical and water. The signal at 0.47 V also decreases in successive scans, indicating that the oxidation of this product leads to further reaction. Simultaneously, a new pair of peaks around 0.17 V grow in, as shown in Figure 7a. The formal potential of this redox couple is within the range of electroactivity of quinone/hydroquinone systems.

Thus, the reaction of anthracene with water likely leads to the formation of hydroxyanthracenes and anthraquinones. It is well-known that the most stable anthraquinones are those having two carbonyl groups on the same (aromatic) ring.[45] The most likely oxidation products are the (9,10), (1,4), and (1,2) isomers. We have recorded cyclic voltammograms of two anthraquinones: 1,4-anthracenedione and 9,10-anthracenedione (Figure 7b, scans ii and iii, respectively). The formal potential of the 1,4-anthracenedione/1,4-dihydroxyanthracene redox couple (0.14 V) is very close to that of the oxidation product of surface-bound anthracene, whereas the potential of the 9,10 isomers is shifted ca. 300 mV negative. The formal potential of the 1,2 isomer is known to be 90 mV more positive than that of the 1,4 isomer.[42] On the basis of these data we assign the peak at ~0.17 V to the 1,4 anthracenedione/1,4-dihydroxyanthracene couple.

The chemical nature of the species responsible for the oxidation peak at 0.47 V remains unclear. One possible explanation is (similar to that for pyrene) that the substitution of anthracene with two carbonyl (hydroxyl) groups occurs sequentially rather than simultaneously; hydroxyanthracene is formed first and reacts subsequently to form the dihydroxy/dione species. In this picture, hydroxyanthracene is responsible for the peak at 0.47 V. The putative reactions of covalently bound anthracene are summarized in Scheme 2.

As with pyrene, we can estimate the surface concentration of anthracene on the basis of the amount of charge associated with the oxidation of surface bound species. The charge under peak I (Figure 7) is associated with oxidation of anthracene and with subsequent oxidation of newly formed products (peaks II and III). We calculate $Q_I - Q_{II} - Q_{III} = 12.3\ \mu C/cm^2$, and dividing it by nF, we obtain the surface concentration of the electroactive species. As with pyrene a significant issue is determining the number of electrons, n, involved in product formation. When only monohydroxyanthracene is created on the surface, $n = 1$, and when dihydroxyanthracene is obtained, the $n = 2$. We could estimate the fraction of anthracene molecules transformed into the mono- or dihydroxy derivative on the basis of Q_{II} and Q_{III} values, but we remain unsure if the hydroxy/quinone derivatives are the only products of anthracene oxidation. The magnitude of the III peak pair is relatively low, which may be the result of some other nonelectroactive products being created that we are not able to detect. We are thus left to place bounds on the surface concentration of anthracene. For n

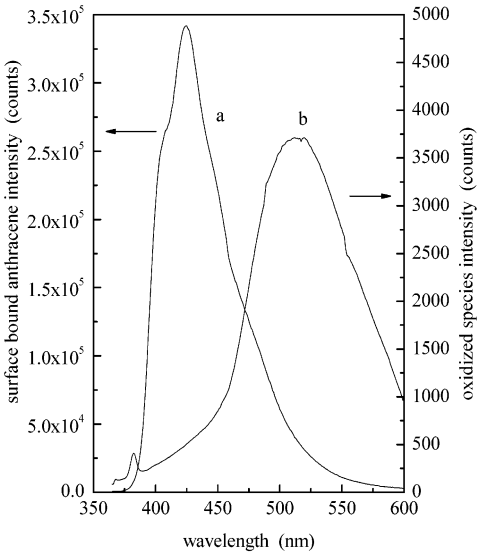

Figure 8. Emission spectra of (a) amidoanthracenehexanoate bound to ITO and (b) products of electrochemical oxidation of amidoanthracenehexanoate bound to ITO.

$= 1$ we obtain $\Gamma_1 = 1.27 \times 10^{-10}$ mol/cm^2 and for $n = 2$, $\Gamma_2 = 0.64 \times 10^{-10}$ mol/cm^2; thus the surface coverage of anthracene on the surface (assuming the concentration of thiol on gold to be 7.7×10^{-10} mol/cm^2 [43]) is not lower than 8.7% and not higher than 16.5%, slightly less than that seen for pyrene covalent deposition.

We now consider the spectral characteristics of the immobilized chromophore as a function of oxidation. Because the emission intensity of any chromophore is quenched efficiently by the presence of a metallic substrate, we attach the molecules to the surface of ITO. We show in Figure 8 the emission spectrum of anthracene bound covalently to ITO through an amide bond. The spectrum (curve a) exhibits a band with a maximum at 410 nm, similar to the data for anthracene on quartz (Figure 6a). The electrochemical oxidation of anthracene on ITO results in disappearance of the emission band (Figure 8b), but no new bands appear in this spectral window. We obtain the same result for irradiation of the sample with UV light in the presence of atmospheric oxygen and water. We have verified that the fluorescence quantum yield of amidoanthracene acetate is much higher (ca. 60×) than that for 1,4-anthracenedione. As mentioned above, it is possible that hydroxyl and quinone derivatives are not the only products of anthracene oxidation, but if such products, exist we are not able to detect them either electrochemically or spectroscopically.

As with pyrene we studied the effect of singlet oxygen on the chromophore molecules. The singlet oxygen was generated by excitation (650 nm) of methylene blue physisorbed on the sample surface. We do not observe any significant changes in the emission spectrum of the surface-bound anthracene as a result of methylene blue irradiation and conclude that singlet oxygen is not involved in photochemical degradation process. Therefore it seems that the electron-transfer mechanism is dominant as the initial step of anthracene oxidation as well.

One of the unusual results obtained from electrochemical data is formation of 1,4- and not 9,10-dione/hydroxyl derivatives. We believe that this result is due to substitution of anthracene with the NHCOOR group, which influences the reactivity of the ring system. Unfortunately, we are not able to determine directly which isomers are generated during the photochemical oxidation, either by emission spectroscopy (no product signal) or by electrochemistry (the signals are probably too small to be detected).

Conclusions

The data we present here for covalently bound pyrene and anthracene reveal a limitation of PAHs as spectroscopic probes of surface adlayers. Such measurements must be performed in oxygen-free and dry environments to prevent the chromophore from manifesting oxidative degradation. The fact that we can achieve such consistent results for two chromophores and three different types of interfaces underscores the generality of the effects we report and rules out the possibility of any anomalous surface enhancement phenomena. It is clear that care must be taken to avoid oxidative degradation in environments characterized by large surface-to-volume ratios.

Acknowledgment. We are grateful to the National Science Foundation for their support of this work through Grant 0090864. M.M. is grateful to the National Science Foundation and NATO for their support of a postdoctoral fellowship (DGE−0209459).

References and Notes

(1) Ulman, A. *An Introduction to Ultrathin Organic Films*; Academic Press: New York, 1991.
(2) Dubois, L. H.; Nuzzo, R. G. *Annu. Rev. Phys. Chem.* **1992**, *43*, 437.
(3) Bain, C. D.; Troughton, E. B.; Tao, Y. T.; Evall, J.; Whitesides, G. M.; Nuzzo, R. G. *J. Am. Chem. Soc.* **1989**, *111*, 321.
(4) Bain, C. D.; Whitesides, G. M. *Angew. Chem., Int. Ed. Engl.* **1989**, *28*, 506.
(5) Ulman, A. *Chem. Rev.* **1996**, *96*, 1533.
(6) Langmuir, I. *J. Am. Chem. Soc.* **1917**, *39*, 1848.
(7) Blodgett, K. B. *J. Am. Chem. Soc.* **1935**, *57*, 1007.
(8) Allara, D. L.; Nuzzo, R. G. *Langmuir* **1985**, *1*, 45.
(9) Allara, D. L.; Nuzzo, R. G. *Langmuir* **1985**, *1*, 52.
(10) Lee, H.; Kepley, L. J.; Hong, H. G.; Akhter, S.; Mallouk, T. E. *J. Phys. Chem.* **1988**, *92*, 2597.
(11) Hong, H. G.; Sackett, D. D.; Mallouk, T. E. *Chem. Mater.* **1991**, *3*, 521.
(12) Katz, H. E.; Scheller, G.; Putvinski, T. M.; Schilling, M. L.; Wilson, W. L.; Chidsey, C. E. D. *Science* **1991**, *254*, 1485.
(13) Vermeulen, L. A.; Thompson, M. E. *Nature* **1992**, *358*, 656.
(14) Kohli, P.; Blanchard, G. J. *Langmuir* **2000**, *16*, 4655.
(15) Major, J. S.; Blanchard, G. J. *Chem. Mater.* **2002**, *14*, 2574.
(16) Schlenoff, J. B.; Laurent, D.; Ly, H.; Stepp, J. *Adv. Mater.* **1998**, *10*, 347.
(17) Dubas, S. T.; Schlenoff, J. B. *Macromolecules* **1999**, *32*, 8153.
(18) Schlenoff, J. B.; Laurent, D.; Ly, H.; Stepp, J. *Chem. Eng. Technol.* **1998**, *21*, 757.
(19) Schlenoff, J. B.; Ly, H.; Li, M. *J. Am. Chem. Soc.* **1998**, *120*, 7626.
(20) Schlenoff, J. B.; Dubas, S. T. *Macromolecules* **2001**, *34*, 592.
(21) Caruso, F.; Lichtenfeld, H.; Donath, E.; Mohwald, H. *Macromolecules* **1999**, *32*, 2317.
(22) Feiler, A.; Plunkett, M. A.; Rutland, M. W. *Langmuir* **2003**, *19*, 4173.
(23) Wang, L. Y.; Schonhoff, M.; Mohwald, H. *J. Phys. Chem. B* **2002**, *106*, 9135.
(24) Finklea, H. O. In *Electroanalytical Chemistry*; Bard, A. J., Rubenstein, J., Eds.; Marcel Dekker: New York, 1996; Vol. 19, p 109.
(25) Xia, Y. N.; Whitesides, G. M. *Annu. Rev. Mater. Sci.* **1998**, *28*, 153.
(26) Schvartzman, M.; Sidorov, V.; Ritter, D.; Paz, Y. *J. Vac. Sci. Technol. B* **2003**, *21*, 148.
(27) Sheen, C. W.; Shi, J.-X.; Martensson, J.; Parikh, A. N.; Allara, D. L. *J. Am. Chem. Soc.* **1992**, *114*, 1514.
(28) Sagiv, J. *J. Am. Chem. Soc.* **1980**, *102*, 92.
(29) Major, J. S.; Blanchard, G. J. *Chem. Mater.* **2002**, *14*, 4320.
(30) Karpovich, D. S.; Blanchard, G. J. *J. Phys. Chem.* **1995**, *99*, 3951.
(31) Karpovich, D. S.; Blanchard, G. J. *Langmuir* **1996**, *12*, 5522.
(32) Fatiadi, A. J. *Environ. Sci. Technol.* **1967**, *1*, 570.
(33) Mao, Y.; Thomas, J. K. *Langmuir* **1992**, *8*, 2501.

(34) Reyes, C. A.; Medina, M.; Crespo-Hernandez, C.; Cedeno, M. Z.; Arce, R.; Rosario, O.; Steffenson, D. M.; Ivanov, I. N.; Sigman, M. E.; Dabestani, R. *Environ. Sci. Technol.* **2000**, *34*, 415.

(35) Sigman, M. E.; Schuler, P. F.; Ghosh, M. M.; Dabestani, R. T. *Environ. Sci. Technol.* **1998**, *32*, 3980.

(36) Dabestani, R.; Ellis, K. J.; Sigman, M. E. *J. Photochem. Photobiol. A* **1995**, *86*, 231.

(37) Ostuni, E.; Chapman, R. G.; Holmlin, R. E.; Takayama, S.; Whitesides, G. M. *Langmuir* **2001**, *17*, 5605.

(38) Zotti, G.; Schiavon, G. *Synth. Met.* **1992**, *47*, 193.

(39) Kelepouris, L.; Krysinski, P.; Blanchard, G. J. *J. Phys. Chem. B* **2003**, *107*, 4100.

(40) Lochmuller, C. H.; Colborn, A. S.; Hunnicutt, M. L.; Harris, J. M. *Anal. Chem.* **1983**, *55*, 1344.

(41) Laviron, E. *J. Electroanal. Chem.* **1979**, *101*, 19.

(42) Moriconi, E. J.; Rakoczy, B.; O'Connor, W. F. *J. Org. Chem.* **1962**, *27*, 2772.

(43) Kuwabata, S.; Fukuzaki, R.; Nishizawa, M.; Martin, C. R.; Yoneyama, H. *Langmuir* **1999**, *15*, 6807.

(44) Berlman, I. B. *Handbook of Fluorescence Spectra of Aromatic Molecules*; Academic Press: New York, 1971.

(45) Boldt, P. Extended quinones. In *Chemistry of the Quinoid Compounds*; Vol. 2, Part 2, p 1431.